Improvement of Corrosion Resistance of Stainless Steel Used in Cooling Water Component by Plasma Electrolysis

Jun Heo[a], Jaewoo Lee[a], and Sung Oh Cho[a*]

Department of Nuclear and Quantum Engineering, Korea Advanced Institute of Science and Technology (KAIST),
Daejeon 34141, Korea
[*]Corresponding author: socho@kaist.ac.kr

1. Introduction

Stainless steel is widely used in various fields due to its remarkable properties including high corrosion resistance, good ductility, and being readily formable. Also, it exhibits remarkable mechanical strength, excellent weldability, and high performance at all temperatures. The typical type used in industrial fields is austenitic stainless steel consisting of 304(L) or 316(L). In nuclear power plants, various components are using stainless steel as a base material. Tube support plates in the secondary loop of the steam generator, turbine blade, moisture separator, and seawater lift pumps are the representative components that use stainless steel.

As well known, the secondary and tertiary loop of the nuclear power plant involves corrosive and abrasive environments. With the secondary loop cooling water environment, its relatively high temperature and pressure with dissolved oxygen and pH controlling additives form the corrosive environments for the components using stainless steel. In the case of tertiary loop utilizing seawater as a cooling water exhibits highly corrosive and abrasive environments as well due to high concentration of salts and abrasive particles in the seawater. Although stainless steel has excellent mechanical strength and high corrosion-resistant properties, with those corrosive and abrasive environments being forced for a long time, it suffers a variety of corrosion and wear problems. DentingA denting problem in the steam generator, cavitation erosion, erosion-corrosion in the turbine blades, general corrosion and pitting corrosion in the seawater lift pump, and Stress Corrosion Cracking (SCC) in the various pipes are the main phenomena occurring.

To improve the corrosion resistance of the stainless steel, previously nanoporous oxide layer formation on the stainless steel surface was studied. It actually improved general corrosion resistance verified with electrochemical characterization showing corrosion potential. But after a long time exposure of the artificial seawater to the nanoporous oxide layer, it was found that corrosion damage penetrated the oxide layer formed. The pores that mitigated volume expansion stress of the growing oxide layer, acted as a corrosive material penetration route so that at a certain point exceeding the threshold concentration of corrosive species induced corrosion failure.

In this study, to supplement those problems, Cathodic Plasma Electrolytic Oxidation (CPEO) method will be discussed. CPEO utilizes extremely high pulsed voltages and temperature to form a protective layer on the substrate. In the presence of certain electrolytes, target metals are placed as a working electrode and the counter electrode is electrically connected. Generally, the CPEO process shows a loose porous layer and inner compact layer with great hardness and adhesion. Due absence of nanopores on the surface corrosive species concentration will be blocked efficiently and additional protection from wear attacks can be achieved with excellent hardness. By changing the electrolyte composition and electrical conditions, contemplating the mechanisms of the compact oxide layer formation process will be the main issue of this paper. For this purpose surface morphologies and composition of the fabricated compact oxide layer will be examined.

2. Methodology

2.1 Materials and characterization

A specially designed stainless steel specimen was used for the CPEO experiment. As shown in Fig. 1, the specimen had a circular CPEO target part and handle attached for the electrical connection part. For stainless steel, type 304 was used as it's composed of the basic composition of the most widely used stainless steel. In the case of electrolyte, glycerol (ACS reagent, $\geq$ 99.5 %) was used as an organic solvent and KCl (ACS reagent, 99.0-100.5 %) was used as a conductive material. Deionized (DI) water was also used to dissolve the conductive material into the electrolyte. Before the CEPO process, sonication of the sample in acetone & DI water for 10 min. was conducted and dried in an oven. After the CPEO process, the sample was rinsed with DI water and dried in an oven.

Figure 1. Type 304 stainless steel specimen

After the experiments, the morphology characterization of the specimen was conducted using a field emission scanning electron microscope (FESEM, Hitachi SU5000, Japan), and cross-sectional composition was characterized with the SEM attached Energy Dispersive X-ray Spectroscopy (EDX). The crystalline structure and composition of the specimen were examined using an X-ray diffractometer (XRD, D/MAX 2500 V, Rigaku, Japan).

2.2 Cathodic Plasma Electrolytic Oxidation (CPEO)

Generally, Plasma Electrolytic Oxidation (PEO) process is applied for the valve metals, such as Aluminum, Zirconium, Magnesium, etc. However, in this study, stainless steel should be the target material for plasma electrolysis. In the case of the PEO process of stainless steel necessary surface plasma discharge hardly occurs because of the absence of the insulating stable oxide layer formed on the surface and the driving force of the iron is lower than that of hydrogen. To compensate for those problems, a Cathodic process of PEO was conducted for this study. Stainless steel target was placed as the cathode and the evolved gas-phase envelope on the surface was used as the insulating film for the plasma discharge by breakdown phenomenon. From those gas-phase envelopes, active species such as active oxygen or carbon can combine with the surface-active iron to form oxides resulting in the CPEO process. Fig. 2a is showing the schematic diagram of the CPEO process, and Fig. 2b shows the experimental setup of the CPEO process.
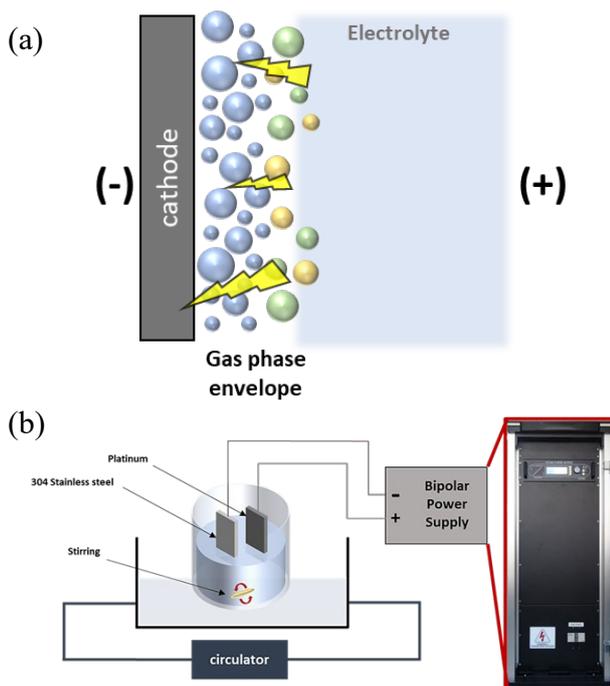

(a)

(b)

Figure 2. Schematic diagram of CPEO(a) and experimental setup (b)

For the experiment, an electrolyte consisting of glycerol, DI water, and KCl was used. The composition ratio of the glycerol was varied from 75 % to 80% and KCl composition was 0.1 M and 0.3 M. Voltage was from 350 ~ 400 V for the positive bias and 0 ~20 V was utilized for the negative bias. Following duty cycle was 45 % and 10 ~45 % each for the positive and negative bias. The frequency of the pulsed input was varied from 100 ~ 2000 Hz and the duration was 2 to 10 min.

3. Results and Discussion

3.1 Surface morphology and composition

Firstly, the frequency variation was conducted The electrolyte composition was fixed as 80 volume % of Glycerol and 20 % of DI water with 0.1 M of KCl. The voltage applied was +350 V and – 0V. The duty cycle was adopted as 45 %. In the case of frequency 300 / 500 / 1000 / 1500 / 2000 Hz was examined for 10 min. each. Fig. 3 shows the surface morphologies of the CPEOed samples at each frequency. It was found that the grains were observable at the moderate frequency of 500 and 1000 Hz. While the others showed non-observable grains on the surface. And in the 1000 Hz sample, it was found that the grain size was finer compared with the 500 Hz sample. With the 2000 Hz sample clearly visible river flow-like structure was characterized while others showed similar structures with smaller sizes. The river flow-like structure was predicted as the molten and solidified iron with extremely high temperatures at the local points. As the frequency increased, the exhibition of those structures was more distinctive.

300 Hz

500 Hz

1000 Hz

1500 Hz

2000 Hz
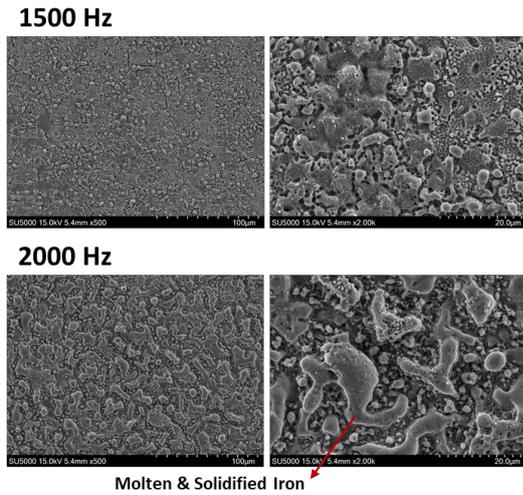

Molten & Solidified Iron
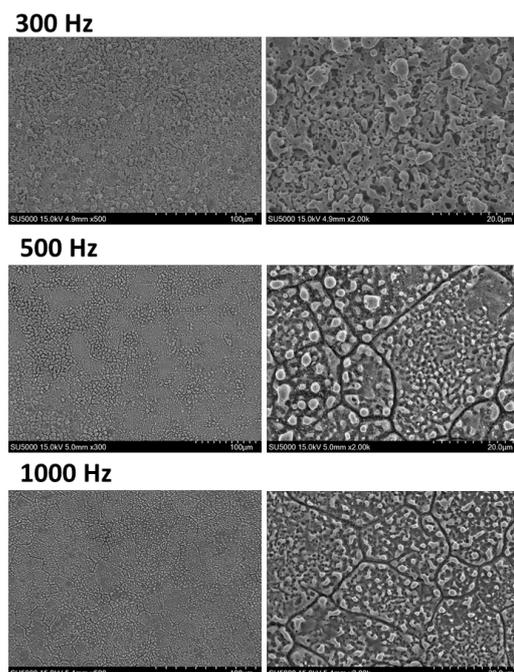
Figure 3. Surface morphologies of frequency variable samples

As shown in surface EDX characterization (Fig. 4) of the 300 / 1000 / 2000 Hz sample, an increase of oxygen contents with increasing frequency was observed. While the carbon contents followed the opposite tendency. In the case of chromium, it tended to increase with the increasing frequency and the iron contents were nearly steady for all cases. It can be explained that the chromium diffusion to the outer surface was enhanced with the increase of frequency. With the increment of oxygen contents by frequency increase, it can be derived from the numbers of discharges. As the frequency increase, the number of discharges at one site decreases but the number of discharges per surface increases which results in increasing the oxide contents. With the above experimental condition, the local heat effect on the sample surface was examined. To overcome this problem, an increase in applied voltage and conductive material ratio with direct use of circulating bath for efficient cooling was conducted.

300 Hz

Element	O	C	Cr	Fe
Atomic %	3.83	39.34	10.33	46.69

1000 Hz

Element	O	C	Cr	Fe
Atomic %	7.26	30.62	21.07	41.05

2000 Hz

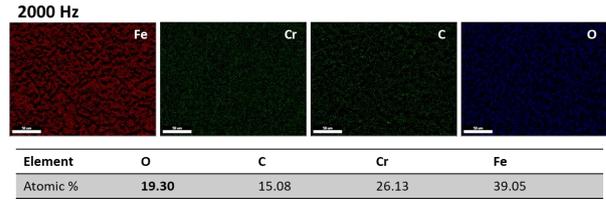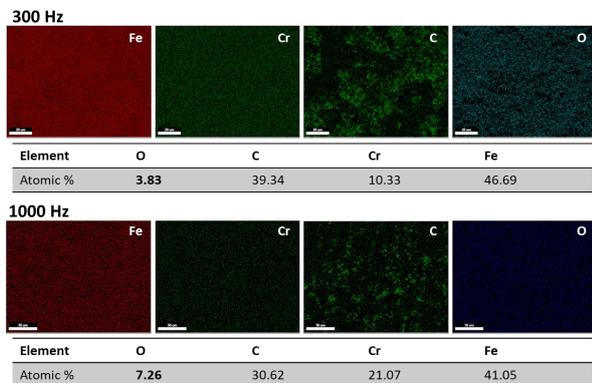| Element	O	C	Cr	Fe
Atomic %	19.30	15.08	26.13	39.05

Figure 4. EDX characterization of frequency variable samples

With the improved condition, again frequency variation was conducted. Glycerol contents of 75 volume % and the DI water rest were used and KCl contents of 0. 3 M was added. The applied voltage was + 400 V and – 20 V each and the duty cycle was +45 % and -45 %. Frequency was adopted as 100 / 200 / 500 Hz with 5 min. duration. The shown morphologies (Fig. 5) of the samples exhibit a more dense structure than the previous samples. In the point of oxygen contents, the 500 Hz sample showed the highest ratio while the second place was the 100 Hz sample. Molten iron eruption and solidification were still observed and the difference was that it showed a more porous structure with the 100 Hz sample but smoother with the high-frequency sample. The interesting part of characterization was that in the moderate frequency sample, chromium oxidation was occurred showing the locally formed oxides as shown in the EDX image. Those chromium oxide formations can serve benefits in the perspective of corrosion protection.
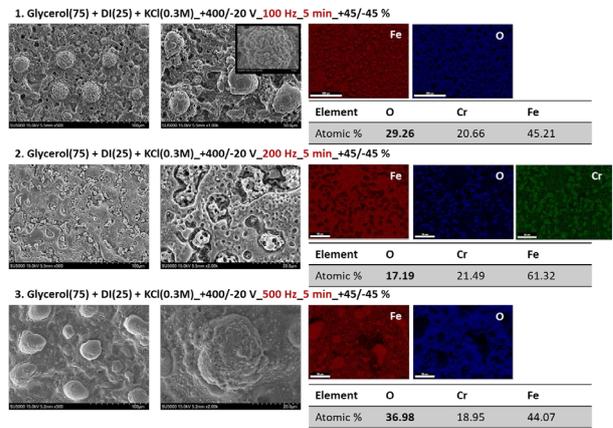
1. Glycerol(75) + DI(25) + KCl(0.3M)_+400/-20 V_100 Hz_5 min_+45/-45 %

Element	O	Cr	Fe
Atomic %	29.26	20.66	45.21

2. Glycerol(75) + DI(25) + KCl(0.3M)_+400/-20 V_200 Hz_5 min_+45/-45 %

Element	O	Cr	Fe
Atomic %	17.19	21.49	61.32

3. Glycerol(75) + DI(25) + KCl(0.3M)_+400/-20 V_500 Hz_5 min_+45/-45 %

Element	O	Cr	Fe
Atomic %	36.98	18.95	44.07

Figure 5. Surface morphologies and compositions of the CPEOed samples with improved conditions

3.2 Cross-sectional morphology and composition

Cross-sectional morphology was characterized with the sample having a condition of 75 % of Glycerol, 25 % DI water, and 0.3 M of KCl. Voltage was +400 and -20 V with a duty cycle of +45 and – 30 %. Frequency was adopted as 100 Hz for 5 min. duration. As shown in Fig. 6, the porous loose layer was nearly observable and the compact layer was mainly observed.

In the middle of the oxide layer, spherical molten and solidified iron was observed which was stuck in the oxide layer before the eruption to the surface. With line spectrum through the depth of the oxide layer showed the distinct oxide layer region with clearly increased oxygen contents. Also, the chromium contents showed a high proposition as consent with the previous results.

Glycerol(75) + DI(25) + KCl(0.3M)_+400/-20 V_100 Hz_5 min_+45/-30 %
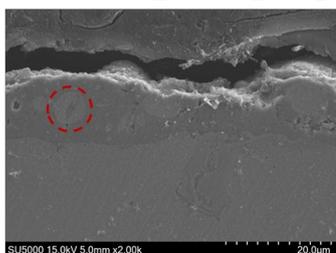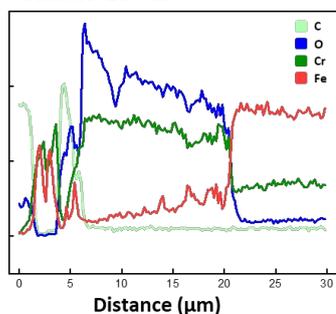

Thickness: 16.4 um

Figure 6. Cross-sectional morphology and composition

3.3 Crystalline structure

XRD patterns were characterized with the negative duty cycle variation samples of -20 / -30 / -45 %. The first one with the -20 % duty cycle showed the crystalline structure of mainly austenite structure. The formed oxide layer was characterized as magnetite phase as shown in all samples. The interesting part was that base austenite phase peaks were weakened as the negative duty cycle increased. Perhaps, it can be explained that an increase in the negative duty cycle enhanced the formation of the oxide layer so that the austenite from the base substrate was hard to be characterized. In consent with the above-mentioned information, chromium oxide (CrO_2) was also found in the peaks. Those chromium oxides can be beneficial for corrosion protection, resulting in a demand for corrosion resistance inspection.
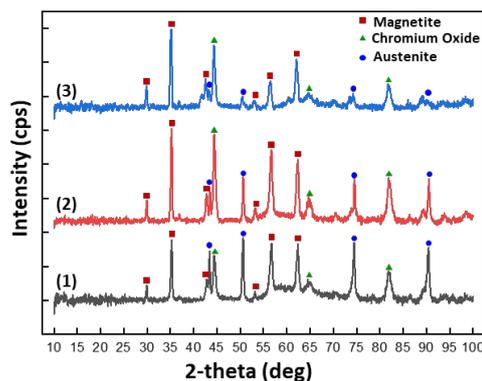
(1) Glycerol(75) + DI(25) + KCl(0.3M)_+400/-20 V_100 Hz_5 min_+45/-20 %

(2) Glycerol(75) + DI(25) + KCl(0.3M)_+400/-20 V_100 Hz_5 min_+45/-30 %

(3) Glycerol(75) + DI(25) + KCl(0.3M)_+400/-20 V_100 Hz_5 min_+45/-45 %

Figure 7. XRD patterns of duty cycle variable samples

4. Conclusion

To improve the corrosion resistance of the main material used for the cooling water components in the nuclear power plants, the CPEO process was tested to fabricate the protective oxide layer on the metal surface. By varying the experimental conditions of the CPEO, the morphologies, composition, and crystalline structures were characterized. In a variation of frequency, moderate frequency showed clear grains on the surface. The molten and solidified irons were basically observed on the surface of all samples, but it was distinctive with the higher frequency sample. And EDX characterization showed that the increase in frequency also increased the oxygen contents of the oxide layer with an increment of discharge numbers per surface. After such a trial, to compensate for the local heat problem, the voltage and conductive material ratio were increased. Then the surface morphologies showed smoother surface and interestingly chromium oxides were found which can be beneficial to the corrosion protection layer. With XRD pattern examination, mainly austenite peaks were found which were derived from the substrate. For the oxide part, the magnetite phase was found to be the main composition. As consent with the surface inspection, chromium oxides were also found in the patterns. With these mechanism examinations, more progressed steps of CPEO drove corrosion protection layer fabrication can be possible. For further research, a much more stable oxide layer should be fabricated with the optimization of the experimental conditions and the electrochemical corrosion test should also be conducted.

REFERENCES

[1] Clyne, Trevor William, and Samuel Christopher Troughton. "A review of recent work on discharge characteristics during plasma electrolytic oxidation of various metals." *International materials reviews* 64.3 (2019): 127-162.

[2] Darband, Gh Barati, et al. "Plasma electrolytic oxidation of magnesium and its alloys: Mechanism, properties and applications." *Journal of Magnesium and Alloys* 5.1 (2017): 74-132.

[3] Yang, Xu, et al. "Cathodic plasma electrolysis processing for metal coating deposition." *Plasma Chemistry and Plasma Processing* 37.1 (2017): 177-187.

[4] Jin, Xiaoyue, et al. "Characterization of wear-resistant coatings on 304 stainless steel fabricated by cathodic plasma electrolytic oxidation." *Surface and coatings technology* 236 (2013): 22-28.

[5] Jin, Xiaoyue, et al. "Preparation and tribological behaviors of DLC/spinel composite film on 304 stainless steel formed by cathodic plasma electrolytic oxidation." *Surface and Coatings Technology* 338 (2018): 38-44.